Frequency Response of a WG-SACM-APD InGaAs/InP Structure

F. EMAMI and M. FERDOWSIYAN TEHRANI
Electrical and Electronics Engineering
Shiraz University of Technology
Airport road, Shiraz
IRAN
http://www.sutech.ac.ir

Abstract: - A theoretical model of a waveguide avalanche photodiode (WG-APD) for an InGaAs/InP with separate absorption, charge and multiplication (SACM) regions, is presented and its frequency response is surveyed. We studied the carrier velocity differences in the adjacent layers and we showed that there are some variations in the case of non equal carrier velocities for the frequency response of the structure. We also found that the same velocities are considered for all layers if we choose an appropriate thickness for different layers.

Key-Words: - avalanche photodiode, carrier velocity, frequency response, modelling.

1 Introduction

There is a fast growth in communication technology and, hence, we need a large gain bandwidth. In this respect one can use an avalanche photodiode (APD) which has a large gain bandwidth [1]. Using a waveguide photo-detector (WG-PD) together with long absorption length it is possible to achieve a large output current [2]. To increase the gain bandwidth, we employed two distinct layers for absorption and multiplication mechanisms in a WG-APD. In this case, the absorption is realized in the material with lower band gap and the multiplication phenomenon is accomplished in higher gap material [3]. If we insert an excess layer (with high-doped material, which is called charge layer) between these two layers, we can have large gain bandwidth when imposing an applied electric field (Fig. 1). To decrease carrier trapping due to band gap differences between absorption layer and another layers, we can use guiding and grading layers [4], [5].

There are many methods to analyzing the frequency response of APDs [6], [7]. In this paper we study the frequency response of a waveguide separate absorption, charge multiplication APD (WG-SACM-APD) made by InGaAs/InP. It is shown (in references [7], [8] and [9]) that the electron and hole velocities are important parameters in determining the frequency response of the devices. These parameters are different for the layers of InP and InGaAs structures. Using this assumption we calculate the frequency response of the device and compare the results with the case of equal carrier velocities in different layers, which is a usual approximation.

2 Time Response of Detector

The structure of a WG-SACM-APD is shown in Fig.1. Light enters the absorption layer and generates an electron-hole pair (EHP) called primary EHPs. The primary electrons (P.E.) move downward (to N^+ layer) and the primary holes (P.H.) move upward (to P^+ layer). The primary holes moved to P^+ layer are collected, but when the primary electrons reach to multiplication layer they arrive a dead space (with length Δw_m), and generation of secondary EHPs starts. These secondary carriers (named by S.E. and S.H.) move to N^+ and P^+ layers and are collected. The field distribution is shown in Fig.1 [9]. This field divide to two sections; one in the absorption and grading layers and the other in the multiplication layer. Due to this field distribution the carriers have different velocities in different layers. We define these velocities as follow:

v_{p1}; Hole velocity in absorption, charge and grading layers,
v_{n1}; Electron velocity in absorption, charge and grading layers,
v_{p2}; Hole velocity in multiplication layer,
v_{n2}; Electron velocity in multiplication layer.

The time response of primary electrons, $N_{p(t)}$ and primary holes, $p_{p(t)}$ are:

$$N_p(t)=\eta\frac{p_i}{hv}\left\{\left[u(t)-u\left(t-\frac{x_t}{v_{n1}}-\frac{x_m}{v_{n2}}\right)\right]+\left(\frac{x_a+x_t-v_{n1}\left(t-\frac{x_m}{v_{n2}}\right)}{x_a}\right)\times\left[u\left(t-\frac{x_t}{v_{n1}}-\frac{x_m}{v_{n2}}\right)-u\left(t-\frac{x_m}{v_{n2}}-\frac{x_a+x_t}{v_{n1}}\right)\right]\right\} \quad (1)$$

$$P_p(t)=\eta\frac{P_i}{hv}\left\{\left[\frac{x_a-v_p t}{x_a}\right]\times\left[u(t)-u\left(t-\frac{x_a}{v_p}\right)\right]\right\} \quad (2)$$

where x_a and x_m are absorption and multiplication thicknesses respectively; x_t is the sum of charge and grading layer thickness between multiplication and absorption layers and η is the quantum efficiency of the detector.

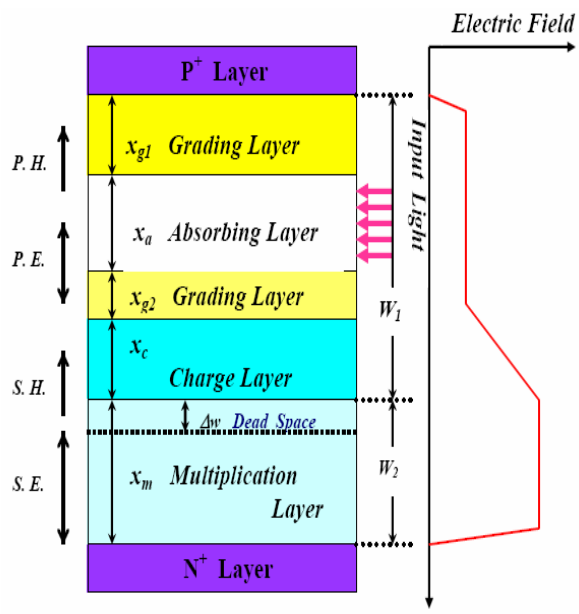

Fig.1 Schematic diagram of a WG-SACM-APD.

Primary electrons move toward the dead space and generate secondary EHPs. Avalanche mechanism forms in the multiplication layer. Mathematically, this process could be computed by convolving the electrons which enter the dead space and the exponential term $\exp[-t/((M_0-1)T_m)]/T_m$, where M_0 is multiplication factor and T_m is the time consuming to avalanche mechanism forms. The time responses of secondary electrons and holes are as follows:

$$\frac{x_a}{v_{n1}}>\frac{x_m-\Delta w_m}{v_{n2}}$$

$$\begin{aligned}N_s(t)=\eta\frac{P_i}{hv}&\times\left\{\frac{V_{n1}t-\Delta w_m(v_{n1}/v_{n2})-x_t}{x_a}\right.\\&\times\left[u\left(t-\frac{x_t}{v_{n1}}-\frac{\Delta w_m}{v_{n2}}\right)-u\left(t-\frac{x_t}{v_{n1}}-\frac{x_m}{v_{n2}}\right)\right]\\&+\frac{x_m-\Delta w_m}{x_a}\times\left[u\left(t-\frac{x_t}{v_{n1}}-\frac{x_m}{v_{n2}}\right)-u\left(t-\frac{x_t}{v_{n1}}-\frac{x_a}{v_{n1}}-\frac{\Delta w_m}{v_{n2}}\right)\right]\\&+\frac{x_a+x_t+x_m(v_{n1}/v_{n2})-v_{n1}t}{x_a}\\&\left.\times\left[u\left(t-\frac{x_t+x_a}{v_{n1}}-\frac{\Delta w_m}{v_{n2}}\right)-u\left(t-\frac{x_t+x_a}{v_{n1}}-\frac{x_m}{v_{n2}}\right)\right]\right\}\\&\otimes\left\{\frac{\exp\left[\frac{-t}{(M_0-1)Tm}\right]}{Tm}\right\}\end{aligned} \quad (3)$$

and if $\frac{x_a}{v_{n1}}<\frac{x_m-\Delta w_m}{v_{n2}}$, the first two terms in the equation (3) must be in the form of:

$$\begin{aligned}&\frac{V_{n1}t-\Delta w_m(v_{n1}/v_{n2})-x_t}{x_a}\\&\times\left[u\left(t-\frac{x_t}{v_{n1}}-\frac{\Delta w_m}{v_{n2}}\right)-u\left(t-\frac{x_t+x_a}{v_{n1}}-\frac{\Delta w_m}{v_{n2}}\right)\right]\\&\times\left[u\left(t-\frac{x_t+x_a}{v_{n1}}-\frac{\Delta w_m}{v_{n2}}\right)-u\left(t-\frac{x_t}{v_{n1}}-\frac{x_m}{v_{n2}}\right)\right]\end{aligned} \quad (4)$$

For secondary holes we have:

$$\begin{aligned}P_s(t)=\eta\frac{P_i}{hv}&\times\left\{\frac{v_{n1}t-(v_{n1}/v_{n2})\Delta w_m-x_t}{x_a}\right.\\&\times\left[u\left(t-\frac{x_t}{v_{n1}}-\frac{\Delta w_m}{v_{n2}}\right)-u\left(t-\frac{x_a+x_t}{v_{n1}}-\frac{\Delta w_m}{v_{n2}}\right)\right]\\&+\left[u\left(t-\frac{x_a+x_t}{v_{n1}}-\frac{\Delta w_m}{v_{n2}}\right)\right.\\&\left.-u\left(t-\frac{x_t}{v_{n1}}-\frac{\Delta w_m}{v_{n2}}-\frac{x_a+x_t}{v_{p1}}-\frac{\Delta w_m}{v_{p2}}\right)\right]\\&+\left(\frac{x_a+x_t+\frac{v_{n1}}{v_{n2}}\Delta w+\frac{v_{n1}}{v_{p2}}\Delta w+\frac{v_{n1}}{v_{p1}}(x_a+x_t)-v_{n1}t}{x_a}\right)\\&\times\left[u\left(t-\frac{x_t}{v_{n1}}-\frac{\Delta w_m}{v_{n2}}-\frac{x_a+x_t}{v_{p1}}-\frac{\Delta w_m}{v_{p2}}\right)\right.\end{aligned}$$

$$-u\left(t-\frac{x_t+x_a}{v_{n1}}-\frac{\Delta w_m}{v_{n2}}-\frac{x_a+x_t}{v_{p1}}-\frac{\Delta w_m}{v_{p2}}\right)\Bigg]\Bigg\}$$

$$\otimes\left\{\frac{\exp\left[\frac{-t}{(M_0-1)T_m}\right]}{T_m}\right\} \tag{5}$$

Now the optical output current I_{ph} in this structure is equal to:

$$I_{ph}(t)=\frac{q(v_{n1}\cdot v_{n2})}{w_1 v_{n2}+w_2 v_{n1}}\left[N_p(t)+N_s(t)\right]+\frac{q(v_{p1}\cdot v_{p2})}{w_1 v_{p2}+w_2 v_{p1}}\left[P_p(t)+P_s(t)\right] \tag{6}$$

where

$$w_1=x_{g1}+x_a+x_t$$
$$w_2=x_m \tag{7}$$

3 Frequency Responses

Frequency responses of the primary and secondary electrons and holes could be found by taking the Fourier transformation of time dependent equations (1)-(5):

$$N_p(\omega)=\eta\frac{P_i}{hv}\left\{\frac{1}{j\omega}+\frac{v_{n1}\left(1-\exp\left(-j\frac{\omega x_a}{v_{n1}}\right)\right)\left(\exp\left(-j\omega\left(\frac{x_t}{v_{n1}}+\frac{x_m}{v_{n2}}\right)\right)\right)}{x_a\omega^2}\right\} \tag{8}$$

$$P_p(\omega)=\eta\frac{p_i}{hv}\left\{\frac{1}{j\omega}+\frac{V_{p1}\left(1-\exp\left(-\frac{j\omega x_a}{V_{p1}}\right)\right)}{x_a\omega^2}\right\} \tag{9}$$

$$N_s(\omega)=\eta\frac{P_i}{hv}\left(\frac{M_0-1}{1+j\omega T_m(M_0-1)}\right)\left(\frac{V_{n1}}{x_a\omega^2}\right)\left[1-\exp\left(-j\omega\left(\frac{x_a}{V_{n1}}\right)\right)\right]\left[\exp\left(-j\omega\left(\frac{x_t}{V_{n1}}\right)\right)\right]\left[\exp\left(-j\omega\frac{x_m}{V_{n2}}\right)-\exp\left(-j\omega\frac{\Delta w_m}{V_{n2}}\right)\right] \tag{10}$$

$$P_s(\omega)=\eta\frac{P_i}{hv}\left(\frac{M_0-1}{1+j\omega T_m(M_0-1)}\right)\cdot\left(\frac{V_{n1}}{x_a\omega^2}\right)\cdot\left[1-\exp\left(-\frac{j\omega x_a}{v_{n1}}\right)\right]\cdot\left[\exp\left(-j\omega\left(\frac{x_t}{v_{n1}}+\frac{\Delta w_m}{v_{n2}}\right)\right)\right]\cdot\left[\exp\left(-j\omega\left(\frac{x_a+x_t}{v_{p1}}+\frac{\Delta w_m}{v_{p2}}\right)\right)-1\right] \tag{11}$$

and also from (6):

$$I_{ph}(\omega)=\frac{q(v_{n1}\cdot v_{n2})}{w_1 v_{n2}+w_2 v_{n1}}\left[N_p(\omega)+N_s(\varpi)\right]+\frac{q(v_{p1}\cdot v_{p2})}{w_1 v_{p2}+w_2 v_{p1}}\left[P_p(\omega)+P_s(\omega)\right] \tag{12}$$

4 Transfer Function

To obtain the transfer function we have to define the optical current I_{opt} which detects the power of input light pulse as follows:

$$I_{opt}=\frac{qp_i}{hv} \tag{13}$$

so, the transfer function will be:

$$H(\omega)=\frac{I_{ph}(\omega)}{I_{opt(\omega)}} \tag{14}$$

where $I_{ph}(\omega)$ and $I_{opt}(\omega)$ are found by (12) and (13) respectively. The detector transfer function is plotted in Fig.2, using the values of table 1.

Table 1

Layer	Material	Thickness
x_a	InP	35 nm
x_m	InGaAs	80 nm
x_c	InP	50 nm
x_{g2}	InP	50 nm
x_{g1}	InP	200 nm
Δw_m	InGaAs	10 nm

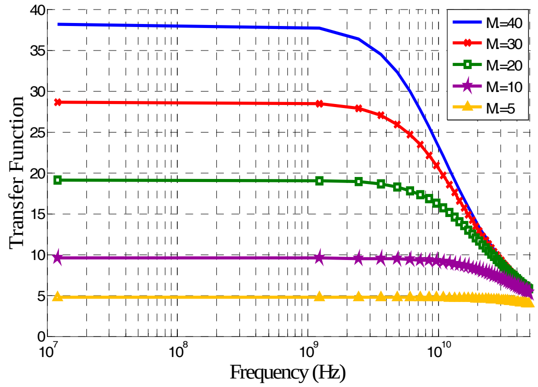

Fig. 2 Transfer functions of a WG-SACM-APD for many values of M_0.

We compare two cases of equal and non equal velocities of carriers in Fig. 3. As shown in the figure, there are some differences for two models.

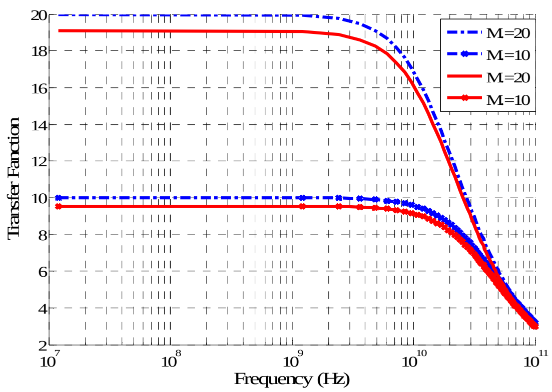

Fig. 3 Transfer function of two models ($v_{n1} = v_{n2}$ and $v_{n1} \neq v_{n2}$) for two values of M_0, the dashed blue curve shows $v_{n1} = v_{n2}$ and the connected red curve shows $v_{n1} \neq v_{n2}$.

By varying the thicknesses of the layers, this difference could be minimized. Figures 4(a) and 4(b) show this point when x_m and x_{g1} vary. When these thicknesses increase it is clear that this difference would be more obvious; so for thicker grading and multiplication layers, we have to impose the non equal velocity condition in our calculations. Variations of the transfer function for x_t and x_a modifications are shown in Fig.5. Now by increasing the aforementioned layer thicknesses, the difference of models could be ignored. But there is a problem in this case. Increasing these layer thicknesses can cause decreasing the bandwidth of the detector. This point is more dominated for lower multiplication gains. Implementation of equal velocities could not be used by decreasing the multiplication thickness because the output current decreases, too. It seems, by lowering x_{g1} there is no such problem, but in this case the trapping of carriers increases (in fact existence of this layer is for elimination of this trapping). So, we have to choose an optimum selection of layer thicknesses.

5 Conclusions

In this paper we studied the frequency response of an InGaAs/InP WG-SACM-APD. We showed that if one considered the same carrier velocities in different layers, there will be a small error in the frequency response of the structure and, hence, in its bandwidths. It is proved that for different thicknesses of layers we can have equal carrier velocity approximations in the different layers of an InGaAs/InP WG-SACM-APD.

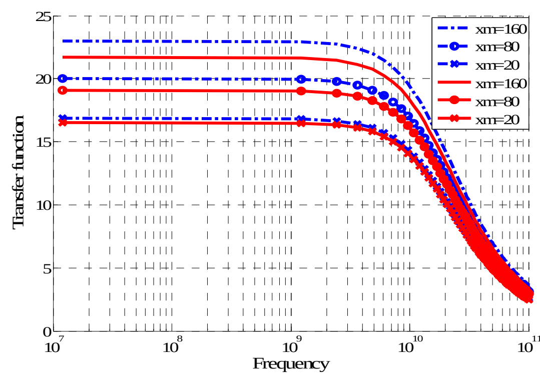

(a)

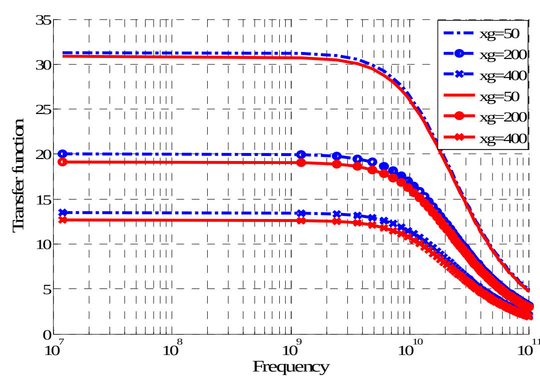

(b)

Fig. 4 Transfer function of two models ($v_{n1} = v_{n2}$ and $v_{n1} \neq v_{n2}$) for different values of (a) x_m and (b) x_{g1}; the dashed blue curve shows $v_{n1} = v_{n2}$ and the connected red curve shows $v_{n1} \neq v_{n2}$.

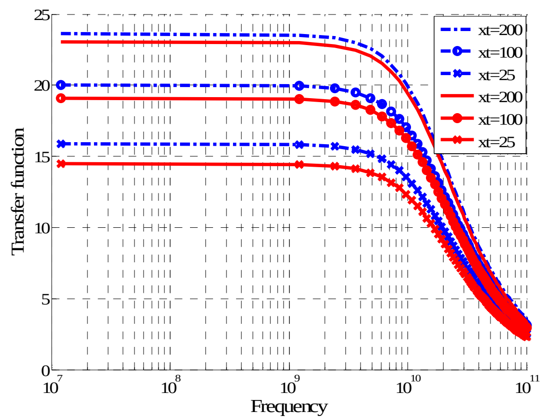

(a)

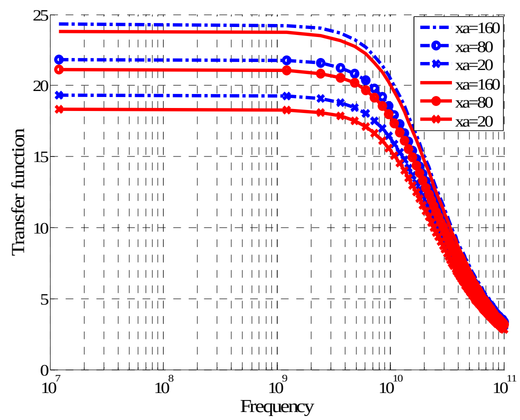

(b)

Fig. 5 Transfer function of two models ($v_{n1} = v_{n2}$ **and** $v_{n1} \neq v_{n2}$ **) for different values of (a)** x_t **and (b)** x_a **; the dashed blue curve shows** $v_{n1} = v_{n2}$ **and the connected red curve shows** $v_{n1} \neq v_{n2}$ **.**

References:

[1] G. S. Kinsey, J. C. Campbell, and A. G. Dentai, "Waveguide avalanche photodiode operating at 1.55 μm with a gain-bandwidth product of 320 GHz," *IEEE Photon. Technol. Lett.*, vol. 13, pp. 842–844, Aug. 2001.

[2] S. Murthy, T. Jung, M. C. Wu, Z. Wang, and W. Hsin, "Linearity improvement in photo-detectors by using index-matching layer extensions," in *Proc. IEEE Lasers &Electro- Optics Soc. 2002 Annu. Meeting*, Nov.2002, pp. 424–425.

[3] S. S. Murtaza, K. A. Anselm, C. Hu, H. Nie, B. G. Streetman, and J. C. Campbell, "Resonant-Cavity Enhanced (RCE) Separate Absorption and Multiplication (SAM) Avalanche Photo-detector (APD)," *IEEE Photon. Technol. Lett.*, vol. 7, no. 12, pp. 1486–1488, Dec. 1995.

[4] J. Wei, F. Xia, and S. R. Forrest, "A high-responsivity high-bandwidth asymmetric twin-waveguide coupled InGaAs-InP-InAlAs avalanche photodiode," *IEEE Photon. Technol. Lett.*, vol. 14, no. 11, pp. 1590–1592, Nov. 2002.

[5] A. Bandyopadhyay, M. J. Deen, L. E. Tarof, and W.Clark "A simplified approach to time-domain modeling of avalanche photodiodes." *IEEE J. Quantum Electron*, vol. 34, pp. 691-699, 1998.

[6] W. Wu, A. R. Hawkins, and J. E. Bowers, "Frequency response of avalanche photo-detectors with separate absorption and multiplication layers," *J. Lightw. Technol.*, vol. 14, no. 12, pp. 2778–2785, Dec. 1996.

[7] Y. M. El-Batawy and M. J. Deen, "Analysis and Circuit Modeling of Waveguide-Separated Absorption Charge Multiplication-Avalanche Photo-detector (WG-SACM-APD)," *IEEE Trans. Electron Devices*, vol. 52, no. 3, pp. 335-344, Mar. 2005.

[8] S. Adachi, *Physical properties of III-V semiconductor compounds, Wiley* USA, 1992.

[9] K. A. Anselm, H. Nie, C. Lenox, P. Yuan, G. Kinsey, J. C. Campbell, and B. G. Streetman, "Performance of thin separate absorption, charge, and multiplication avalanche photodiodes," *IEEE J. Quantum Electron.*, vol. 34, no. 3, pp. 482–490, Mar. 1998.